ISSN: 0067-2904

Preparation of Some New Pyrazine and Triazine Derivatives and Study of their Antimicrobial and Anticancer activities

Assma A. ALAbady , Suaad M. H. Al-Majidi
Department of chemistry, college of science, University of Baghdad, Baghdad, Iraq

Received: 25/1/2023 Accepted: 6/5/2023 Published: 30/5/2024

Abstract

In this study, a new series of 1,2,4-triazine and 1,2-diazine derivatives was prepared in four and three steps, respectively. In the preparation of 1,2,4-triazine derivatives. The first step included a reaction between 2-phenyl-3-aminoquinazoline-4-(3H)-one and chloroacetyl chloride in the presence of Et_3N as a base to produce (**1**) in 83% yield. Compound (**1**) was then reacted in the second step with hydrazine hydrate to yield the corresponding hydrazide (**2**) in 80% yield. The third step of our work included a reaction of compound (**2**) with different compounds: α-Naphthan isocyanate to give compound (**3**) (90% yield); phenyl isocyanate to afford compound (**4**) (80% yield); phenyl isothiocyanate to yield compound (**5**) (85% yield); and CS_2 in basic medium to provide compound (**9**) in 85% yield. In the fourth step, the products (**3**-**5**) were then cyclized in alkaline medium to give substituted trizines as six-membered rings (**6**-**8**) in 78-85% yields. The reaction of compound (**9**) with hydrazine hydrate afforded compound (**10**) in 80% yield. In the preparation of 1,2-diazine derivatives, compound (**2**) was treated with cyclic and aromatic anhydrides to give (**11**-**15**) in yields ranging from 75 to 86%. The prepared compounds were characterized by FT-IR, ^{13}C NMR, and ^{1}H NMR spectroscopy and measured for a number of their physical characteristics. Also, certain tests have been performed on their anti-microbial activities on fungal strains, bacterial strains, and gram-negative and gram-positive bacteria for the identification of the most sufficient of the biologically active complexes. Finally, the anticancer activity of three prepared compounds (**2**, **12**, and **13**) was tested, and the results showed good effects of these compounds against prostate cancer PC3.

Keywords: 2-Phenyl-3-amino qinazoline-4(3H)-one, Pyridazine, 1,2,4-Triazine,prostate cancer PC3, Anti-microbial.

تحضير بعض مشتقات بايرازين وترايازين الجديدة ودراسه فعاليتها المضادة للمايكروبات والمضادة للسرطان

اسماء عباس العبادي * ، سعاد حسين الماجدي
قسم الكيمياء، كلية العلوم، جامعة بغداد، بغداد، العراق

الخلاصة

في هذه الدراسة، تم تحضير سلسلة جديدة من مشتقات 4,2,1 –ترايازين و 2,1 – دايازين من خلال ثلاث و اربع خطوات على التوالي . في تحضير مشتقات 4,2,1 –ترايازين . تضمنت الخطوة الاولى تفاعل

*Email: asmaaabbas353@gmail.com

بين 2–فنيل–3–امينو كوينازولين–4– (3H)– اون و كلورو اسيتيل كلورايد بوجود Et_3N كقاعدة للحصول

على المركب **(1)** بمنتوج 83 %. ثم تفاعل مركب **(1)** في الخطوة الثانية مع الهيدرازين المائي للحصول على مركب الهايدرازايد **(2)** بمنتوج 80%. تضمنت الخطوة الثالثة من العمل بتفاعل المركب **(2)** مع مركبات مختلفة: α– نفثل ايزوسيانات للحصول على المركب **(3)** بنسبة 90%: و فنيل ايزوسيانات للحصول على مركب **(4)** بمنتوج 80%: فنيل ايزوثايوسيانات للحصول على مركب **(5)** و بمنتوج 85%: و CS_2 في وسط قاعدي للحصول على المركب **(9)** بمنتوج 85% . في الخطوة الرابعة المركبات من **(3)** الى **(5)** تم غلقهافي وسط قاعدي للحصول على حلقات سداسية معوضة للمركبات من بحلقات سداسية(6–8) وبمنتوج من 78 الى 85% . تفاعل المركب **(9)** مع الهيدرازين المائي للحصول على المركب **(10)** و بمنتوج 80% . حضرت مشتقات 2,1–دايازين من المركب **(2)** بمعاملتها مع انهيدريدات اروماتية وحلقية للحصول على المركبات **(11–15)** وبمدى منتوج من 75 الى 86% تم تشخيص جميع المركبات التي تم تحضيرها بواسطة التقنيات الطيفية FT–IR, ^{1}H NMR, ^{13}C NMR و كذلك قيست خواصها الفيزيائية. تم اختبار فعالياتها المضادة للبكتريا و للفطريات. واخيرا، تم اختبار الفعالية المضادة للسرطان لثلاث من المركبات التي تم تحضيرها **(2** ,**12**, **13)** واظهرت النتائج فعالية تثبيطية جيدة لهذه المركبات ضد سرطان البروستات PC3.

1. Introduction

Pyridazine can be defined as a heterocyclic organic compound with the molecular formula $(CH)_4N_2$ [1]. It is an aromatic six-membered ring that has two neighboring nitrogen atoms [2]. It has two other tautomeric forms, pyrazine and pyrimidine [3]. The diazine derivatives have gained a great deal of attention in the present day as a result of their many advantageous traits. For instance, the ease with which structural alterations can be made [4], the excellent electrical and optical properties [5], and the beneficial biological activities [6]. The pyridazine, which has been known as the "wonder nucleus", as well as its derivatives, were reported because of their biological and chemical actions to have a broad variety of biological activities [7], which include potent and anti-hypertensive cardiotonic agents [8]. In addition, in their anti-HAV assessment [9]' a variety of pyridazine-based heterocyclic scaffolds were used in the newest programs of medicinal chemistry against various biological targets and with different physiological effects and were used for anti-inflammatory activity and inhibition [10], anti-cancer [11], anti-tuberculosis [12], anti-microbial and antioxidant [13], anti-tumor [14], anti-proliferative [15] and anti-viral [16]. The pyridazine ring represents part of the structure of some of the therapeutic agents that are found on the market, which include minaprine, cadralazine, pipofezine, and hydralazine [17]. 1,2,4-Triazine is a six-membered ring that bears three nitrogen atoms. Some time ago, this system was referred to as triazines (asymmetrical triazines) as well [18]. 1,2,4-Triazine and its derivatives represent a significant heterocyclic compound class, which is why they were reported to have a broad range of biological activities [19], which include antimalarial agents [20], anti-cancer and antioxidant activities [21], anti-inflammatory agents [22], antimicrobial agents [23], and antibacterial and antiviral agents [24].

2. Materials and methods

2.1. Instruments and chemicals

All the chemicals utilized were purchased from Aldrich, Fluka, and PDH companies. The melting points were measured using gallenkamp in the open capillary glass with the use of the Thomas capillary MP apparatus. FT-IR spectral data were recorded on a Shimadzu FT-IR-8400 using a KBr disc. The ^{13}C NMR and ^{1}H NMR spectral data were recorded using a 500 MHz spectrometer. Chemical shifts are expressed in ppm downfield from tetramethylsilane (TMS) as an internal standard or deuterated DMSO in ^{1}H NMR as a reference. UV-Visible

spectra were recorded by the Shimadzu spectrophotometer and a pel PD-303-spectrophotometer, Japan.

2.2. Synthesis

*2.2.1. 2-chloro-N-(4-oxo-2-phenylquinazolin-3(4H)-yl)acetamide (**1**) [25]*

In a 50-mL round-bottom flask, a mixture of 2-phanyl-3-amino-quinazoline-4(3H)-one (0.5 g, 0.002 mol) and triethyl amine (0.2 mL, 0.0129 mol) in THF (8 mL). This mixture was cooled to 0 °C before adding chloroacetyl chloride (0.12 ml) and stirred for 2 hours at room temperature. The temperature was then raised gradually to 75-85 ^{o}C for 10 hours. After the reaction was complete, ice water was added. The solid crude material was filtered, washed by water, and recrystallized from acetone. The physical characteristics and FT-IR spectral data of compound (**1**) are listed in Table 1.

*2.2.2. 2-Hydrazineyl-N-(4-oxo-2-phenylquinazolin-3(4H)-yl)acetamide (**2**) [26]*

To a solution of compound (**1**) (0.66 g, 0.002 mol) in absolute ethanol (4.0 mL), an excess of hydrazine hydrate (99%) was added before refluxing for 8 hours. After the reaction was complete, the mixture was allowed to cool to room temperature before adding ice water. The solid crude material was then filtered, washed with water, and recrystallized from ethanol and water. Table 1 displays the physical properties and FT-IR spectral data of compound (**2**).

*2.2.3.N-(naphthalen-1-yl)-2-(2-oxo-2-((4-oxo-2-phenylquinazolin-3(4H)-yl)amino)ethyl) hydrazine-1-carboxamide (**3**);2-(2-oxo-2-((4-oxo-2-phenylquinazolin-3(4H)-yl)amino)ethyl)-N-phenylhydrazine-1-carboxamide(**4**); N-(4-oxo-2-phenylquinazolin-3(4H)-yl)-2-(2-(phenylcarbamothioyl)hydrazineyl)acetamide (**5**) [27]*

In a round bottom flask, a mixture of compound (**2**) (0.3 g, 0.001 mol) and phenyl isocyanate (0.1 mL, 0.001 mol), α-naphthyl isocyanate (0.14 mL, 0.001 mol) or phenyl isothiocyanate (0.18 mL, 0.001 mol) in absolute ethanol (10 mL). This mixture was heated to reflux for 5-6 hours. The reaction mixture was then allowed to cool to room temperature, and the solid material was filtered, dried, and recrystallized from the acetone. The physical characteristics and FT-IR spectral data of compounds (**3**-**5**) are shown in Table 2.

*2.2.4.3-((3-hydroxy-4-(naphthalen-1-yl)-1,4-dihydro-1,2,4-triazin-5-yl)amino)-2-phenyl quinazolin-4(3H)-one (**6**),3-((3-hydroxy-4-phenyl-1,4-dihydro-1,2,4-triazin-5-yl)amino)-2-phenylquinazolin-4(3H)-one(7);3-((3-mercapto-4-phenyl-1,4-dihydro-1,2,4-triazin-5-yl) amino)-2-phenylquinazolin-4(3H)-one (**8**) [27]*

Compounds (**3**-**5**) (0.001 mol) in a solution of sodium hydroxide (20 mL, 4.0 N) were refluxed for 5-6 hours. The mixture was then allowed to cool to room temperature and neutralized by HCl (50%). The solid crude material was then filtered and recrystallized from the ethanol. The physical properties and FT-IR spectral data of compounds (**6**-**8**) are listed in Table 6.

*2.2.5.2-(2-oxo-2-((4-oxo-2-phenylquinazolin-3(4H)-yl)amino)ethyl)hydrazine-1-carbodithioate (**9**)[27]*

To a mixture of hydrazide derivative (**2**) (0.3 g, 0.001 mol) and potassium hydroxide solution (0.05 g, 0.001 mol) in absolute ethanol (10 mL), CS_2 (0.6 mL, 0.001 mol) was slowly added to this mixture. The reaction mixture was stirred at room temperature overnight. The solid crude material was then filtered, washed with dry diethyl ether. The crude material of (**9**) was used in the next step without purification. The physical properties of compound (**9**) are listed in Table 7.

*2.2.6. 3-((4-Amino-3-mercapto-1,4-dihydro-1,2,4-triazin-5-yl)amino)-2-phenyl quinazolin-4(3H)-one (**10**) [27]*

In a round bottom flask, a mixture of compound (**9**) (0.4 g, 0.0016 mol) and hydrazine hydrate (4 mL, 0.12 mol, 99%) was refluxed until the hydrogen sulfide evolution had been stopped. The reaction mixture was then allowed to cool to room temperature and acidified with HCl solution (10%) to produce a pale brown precipitate in the mixture. The solid crude material was then filtered and recrystallized from ethanol. The physical properties of compound (**10**) are listed in Table 7.

*2.2.7.2-(5-Methyl-3,6-dioxo-3,6-dihydropyridazin-1(2H)-yl)-N-(4-oxo-2-phenylquinazolin-3(4H)-yl)acetamide(**11**); 2-(8-nitro-1,4-dioxo-3,4-dihydrophthalazin-2(1H)-yl)-N-(4-oxo-2-phenylquinazolin-3(4H)-yl)acetamide(**12**);3,7-dioxo-1,2-diazepan-1-yl)-N-(4-oxo-2-phenylquinazolin-3(4H)-yl)acetamide(**13**);2-(1,4-dioxo-5,6,7,8-tetraphenyl-3,4-dihydrophthalazin-2(1H)-yl)-N-(4-oxo-2-phenylquinazolin-3(4H)-yl)acetamide(**14**);N-(4-oxo-2-phenylquinazolin-3(4H)-yl)-2-(1,4,6,9-tetraoxo-8-(2-(4-oxo-2-phenylquinazolin-3(4H)-yl)acetamido)-3,4,6,7,8,9hexahydropyridazino[4,5-g]phthalazin-2(1H)-yl)acetamide (**15**)[28]*

A mixture of compound (**2**) (0.3 g, 0.001 mol.) and citraconic anhydride, 3-nitrophthalic anhydride, glutaric anhydride, tetraphenylphthalic anhydride, or 1,2,4,5-benzenetetracarboxylic-1,2:4,5-dianhydride (0.001 mol) in glacial acetic acid (10 mL) was refluxed for 6-8 hours. The mixture was then allowed to cool to room temperature before adding ice water, and the solid crude material was filtered and recrystallized from ethanol. The physical properties of compounds (**11**-**15**) are listed in Table 8.

3. Results and discussion

3.1. Chemistry

A new series of pyrazine and 1,2,4-triazine derivatives were synthesized through several sequential reactions. The preparation of these derivatives is shown in Scheme 1. The product 2-phenyl-3-(chloroacetoamide)-quinazoline-4(3H)-one (**1**) was produced *via* the reaction of 2-phenyl-3-aminoquinazoline-4(3H)-one with chloroacetyl chloride in the presence of Et_3N as a base. This compound was diagnosed by FT-IR spectroscopy (Table 1), which shows the disappearance of the NH_2 band and the appearance of absorption bands of new N-H at 3271 cm^{-1}, C=O amide (1687-1658 cm^{-1}), and C-Cl (761 cm^{-1}). This compound was also diagnosed by ^1H NMR spectroscopy (Table 2), which showed a singlet signal at 3.34 ppm owing to two protons of CH_2-Cl, multiple signals at 7.20-8.64 ppm due to aromatic protons, and a singlet signal at 8.74 ppm belonging to the N-H proton. The ^{13}C NMR spectral data of compound (**1**) are displayed in Table 2. In the second step, compound (**1**) was reacted with hydrazine hydrate in absolute ethanol to form 2-phenyl-3-(hydrazinoacetoamide)-quinazoline-4(3H)-one (**2**) in 80% yield. The FT-IR spectrum of this compound indicated the disappearance of the C-Cl absorption at 761 cm^{-1} from the spectrum of compound (**1**). On the other hand, the appearance of the asymmetric and symmetric stretches of NH_2 absorption at 3436 cm^{-1} and 3423 cm^{-1}, respectively. Also, the presence of a strong, sharp band at 3272 cm^{-1}, and C=O at 1683 and 1656 cm^{-1}. The ^1H NMR spectrum of compound (**2**) showed a singlet signal at 3.43 ppm due to CH_2 protons; two separated signals at 4.70 and 6.20 ppm are due to NH and NH_2 protons of $NHNH_2$; multiple signals at 7.20-8.75 ppm belong to aromatic protons; and a singlet signal at 10.02 ppm for the NH-C=O proton. The ^{13}C NMR spectral data of compound (**2**) are displayed in Table 2. Compound (**2**) was then reacted with three reagents (α-naphthyl isocyanate, phenyl isocyanate, and phenyl isothiocyanate to afford the products (**3**-**5**). The FT-IR spectral data of these compounds (**3**-**5**), which showed absorption bands at 3295-3271 cm^{-1} attributed to the N-H band, and 1728-1672 cm^{-1} for C=O amide. On the other hand, the

disappearance of NH_2 absorption for the hydrazide derivative (**2**), and the appearance of a new band of absorption at 1450 cm^{-1} was appeared due to C=S of compound (**5**) (Table 3). The ^1H NMR spectrum of compound (**3**) showed a singlet signal at 3.36 ppm due to CH_2 protons, a singlet signal at 4.13 ppm due to the NH-CH_2 proton, multiple signals ranging from 7.27 to 8.26 ppm for aromatic protons, and multiple signals at 9.03-9.52 ppm for the H-N=C=O proton (Table 4). The ^1H NMR spectrum of compound (**5**) showed a singlet signal at 3.37 ppm due to CH_2-C=O protons, 4.87 ppm for CH_2-NH proton, multiple signals at 7.31-8.61 ppm for fourteen proton of aromatic rings, a singlet signal at 9.81 ppm for H-N-C=O proton, and a singlet signal at 10.52 ppm for H-N-C=S proton (Table 4). The ^{13}C NMR spectral data of compound (**5**) are shown in Table 4. The cyclization reaction of compounds (**3**-**5**) in basic conditions (NaOH, 4.0 N) gave the products (**6**-**8**) in 78-85% yields. The FT-IR spectra of these products (**6**-**8**) showed the disappearance of thiocarbonyl and carbonyl amide group absorptions from the FT-IR spectra of compounds (**3**-**5**), which is an indicator of the conversion to afford compounds (**6**-**8)**. In addition, the appearance of absorptions at 3431-3377 cm^{-1} for the O-H group at compounds (**6** and **7**), respectively. The appearance of N-H absorption at 3281 and 3244 cm^{-1} in compound (**6**), 3298 and 3224 cm^{-1} in compound (**7**), and 3281 and 3242 cm^{-1} in compound (**8**). All details of the FT-IR spectral data for compounds (**6**-**8**) are listed in Table 5. The ^1H NMR spectrum of compound **6** showed a singlet signal at 3.36 ppm due to the N-H proton, a singlet signal at 6.66 ppm due to the C=C-H triazine ring proton, multiple signals at 7.15-8.15 ppm due to the aromatic ring protons, singlet signals at 8.79 ppm for the N-H triazine ring proton, and a singlet signal at 9.50 ppm for the O-H proton (Table 6). The ^{13}C NMR spectral data of compound (**5**) are listed in Table 6. The ^1H NMR spectrum of compound (**8**) showed a singlet signal at 3.36 ppm due to the S-H proton, a singlet signal at 4.13 ppm due to the N-H proton, a singlet signal at 6.67 ppm due to the C=C-H triazine ring proton, multiple signals at 7.19 to 8.08 ppm due to fourteen protons of aromatic rings, and a singlet signal at 9.50 ppm due to the N-H triazine ring proton (Table 6). The ^{13}C NMR spectral data of compounds (**6** and **8**) are listed in Table 6. The reaction of hydrazide derivative (**2**) with CS_2 in KOH/ethanoic was then achieved successfully to afford the corresponding dithiocarbamate salt (**9**), which was then cyclized with hydrazine hydrate (99%) to give 1,2,3-triazine derivative (**10**) in 80% yield. The FT-IR spectra of compound (**9**) showed absorption at 1450 cm^{-1} due to the C=S group. Compound (**10**) showed absorption at 3196 cm^{-1} for the N-H band and two bands at 3276 cm^{-1} and 3249 cm^{-1} for the asymmetric and symmetric stretching, respectively, of the NH_2 group. All FT-IR details of the spectral data for compounds (**9** and **10**) are displayed in Table 7. Compound (**2**) was then reacted with different cyclic and aromatic anhydrides to give the corresponding 1,2-diazine derivatives substituted for *N*-sub-quinazoline-4(3H)-one compounds (**11**-**15**). The FT-IR spectra of these compounds are listed in Table 8, which shows the disappearance of two absorption bands for the asymmetric and symmetric stretching of the NH_2 group and the appearance of the bands at 3434-3307 cm^{-1} due to the N-H band. Two groups of the cyclic carbonyl (C=O amide) at compounds (**11**-**15**) appear at 1753-1730 cm^{-1} and 1697-1662 cm^{-1}.

The ^1H NMR spectral data of compound (**13**) are displays in Table 8, which showed multiple signals from 1.88 to 3.34 ppm due to the six protons of the cyclic CH_2, a singlet signal at 4.70 ppm for the acyclic CH_2, multiple signals at 7.30-8.62 ppm due to the aromatic ring protons, and a singlet signal at 8.65 ppm for two protons N-H bands. The ^{13}C NMR spectral data of compound (**13**) are shown in Table 9.

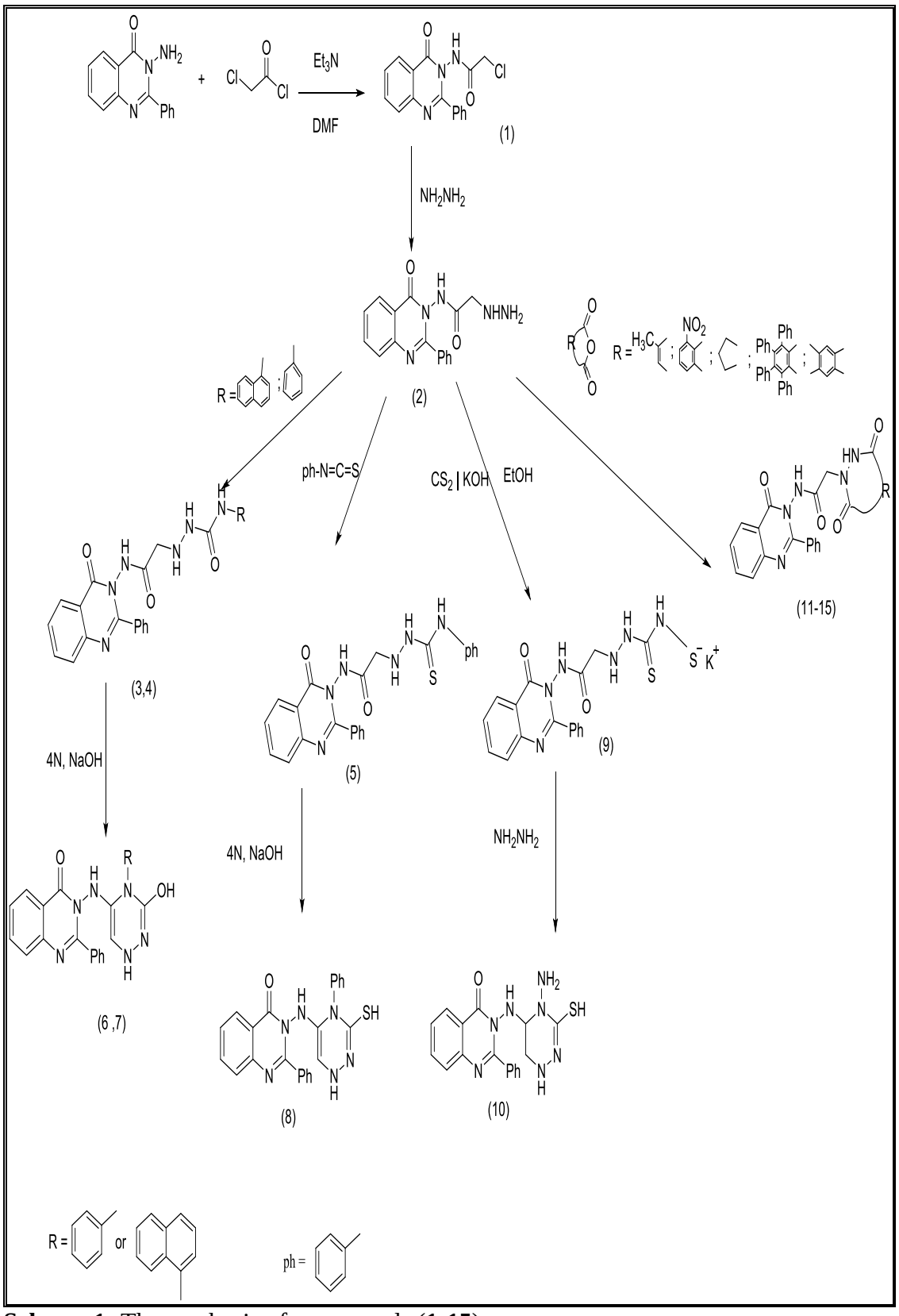

Scheme 1: The synthesis of compounds (**1-15**).

Table 1: Physical characteristics and FT-IR spectral data (υ, cm^{-1}) of compounds (**1** and **2**)

No	Physical characteristics				FT-IR spectral data				
	Structure	m.p. (°C)	Yield (%)	Color	N-H	C-H Aromatic	C=O Amide	C=C Aromatic	Other bands
1	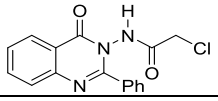	167-168	83	White	3271	3031	1687 1658	1537 1448	761 (C-Cl)
2	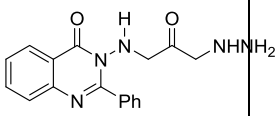	125-126	80	Off white	3272	3026	1683 1656	1589 1450	3436 (asym.) 3423 (sym.) NH_2

Table 2: ^{1}H NMR and ^{13}C NMR spectral data (□ □ ppm) of the compounds (**1** and **2**)

No.	Structure	^{1}H NMR spectral data	^{13}C NMR spectral data
1	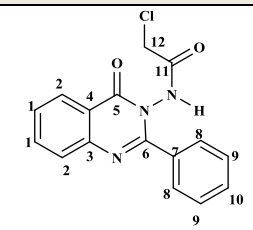	3.34 (s, 2H, CH_2) 7.2-8.64 (m, 9H, Ar-H) 8.74 (s,1H, N-H)	65.6 (C12), 117.1-139.8 and 148.7 (C1, C2, C3, C4, C7-C10), 161.7 (C6), 165.0 (C5 or C11) , 168.1 (C5 or C11)
2	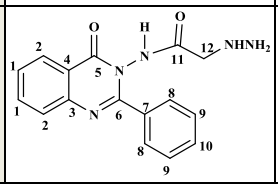	3.34 (s, 2H, CH_2) 4.70 (s, 1H, NH) 6.20 (s, 2H, NH_2) 7.2-8.74 (m, 9H, Ar-H) 10.02 (s, 1H, NH)	65.5 (C12), 117.1-139.7 and 148.7 (C1, C2, C3, C4, C7-C10), 161.7 (C6), 164.8 (C5 or C11), 168.0 (C5 or C11)

Table 3 : Physical characteristics and FT-IR spectral data (□, cm^{-1}) of compounds (**3-5**)

No	Physical characteristics				FT-IR spectral data				
	Structure	m.p. (°C)	Yield (%)	Color	N-H	C-H	C=O	C=C	Other bands
3	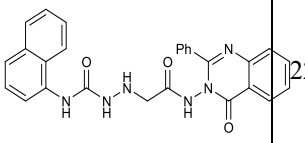	228-229	90	White	3274	3055	1701 1681	1558 1448	C-N 1641
4	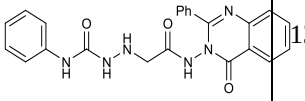	138-140	80	Brown	3295	3099	Overlap 1672	1550 1448	□
5	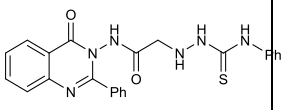	269-270	85	Off white	3271	3014	1728 1683	1542 1448	C-N 1643 C=S 1445

Table 4 : ^{1}H NMR and ^{13}C NMR spectral data (□□ ppm) of compounds (**3** and **5**)

No	structures	^{1}H NMR spectral data	^{13}C NMR spectral data
3	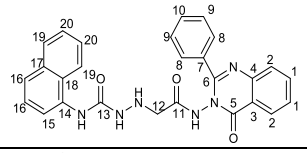	3.36 (s, 2H, CH_2), 4.13 (s, 1H, N-H), 7.27-8.60 (m, 16H, Ar-H), 9.03-9.52 (m, 3H, N-H)	60.8 (C12), 121.2-134.8 (C1, C2, C4, C7-C10, C14-C20), 139.6 (C3), 155.4 (C6), 165.1 (C5), 168.0 (C11 and C13)
5	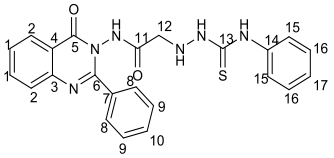	3.37 (s, 2H, CH_2), 4.78 (s, 1H, N-H), 7.13-8.61 (m, 14H, Ar-H), 9.81 (s, 1H, N-H), 10.52 (apparent s, 2H, N-H)	55.8 (C12), 119.1-134.8 and139.82 (C1, C2, C3, C4, C7, C8, C9-C10, C14-C17), (C3), 150.80 (C6), 164.98 (C5 or C11 or C13), 168.10 (C5 or C11 or C13), 178 (C5 or C11 or C13)

Table 5: Physical characteristics and FT-IR spectral data (□, cm^{-1}) of compounds (**6-8**)

No.	Physical characteristics				FTIR absorption spectral data				
	Structure	m.p. (°C)	Yield (%)	Color	N-H	C-H	C=O	C=C	Other bands
6	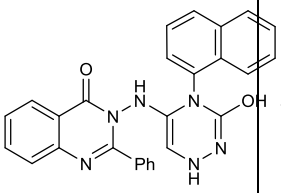	206-207	80	Brown	3281 3244	3053	1681	1558 1444	OH 3431 C=N 1643
7	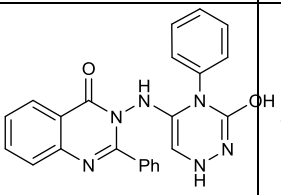	233-235	78	White	3298 3224	3097	1670	1596 1550	OH 3377 C=N 1620
8	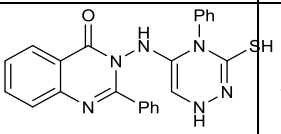	269-270	85	Off white	3281 3242	3051	1679	1601 1481	C=N 1642

Table 6: ^{1}H NMR and ^{13}C NMR spectra data (□, ppm) of compounds (**6** and **8**)

No.	Structure	^{1}H NMR spectral data	^{13}C NMR spectral data
6	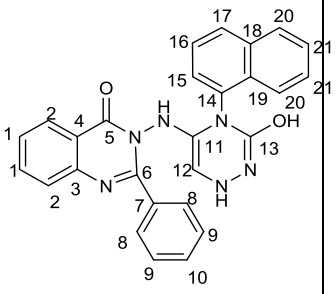	3.36 (s, 1H, N-H), 6.66 (s, 1H, C=C-H), 7.15-8.15 (m, 16H, Ar-H), 8.79 (s, 1H, N-H), 9.50 (s, 1H, O-H)	111.1 (C12), 112.2-138.8 (C1, C2, C4, C7-C10, C14, C15-C21), 147.6 (C11), 148.3 (C3 and C12), 159.7 (C6 and C13), 165.7 (C5)
8	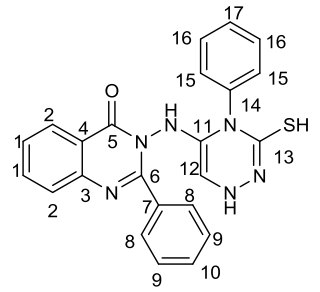	3.36 (s, 1H, S-H), 4.13 (s, 1H, N-H), 6.67 (s, 1H, C=C-H), 7.19-8.08 (m, 14H, Ar-H), 9.50 (s, 1H, N-H)	107.8 (C12), 115.8-139.8 (C1, C2, C4, C7, C10, C14, C15, C21), 145.17 (C3 and C11), 155.36 (C6 and C13), 164.78 (C5)

Table 7: Physical characteristics and FT-IR spectra data (□, cm^{-1}) of compounds (**9** and **10**)

No	Physical characteristics				FT-IR spectral data				
	Structures	m.p (°C)	Yield (%)	Color	N-H	C-H	C=O	C=C	Other bands
9	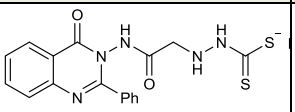	200-201	85	Deep Brown	3251 3178	3041	1701 1681	1554 1458	□C=N 1638 □C=S 1450
10	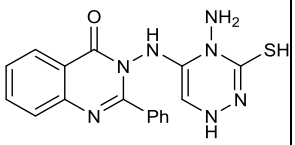	170-171	80	Pale Brown	3196	3043	1704	1562 1498	NH_2 Asym. 3276 Sym. 3249 S-H 2580

Table 8: Physical characteristics and FT-IR spectral data (□, cm^{-1}) of compounds (**11-15**)

No	Structure	m.p. (°C)	Yield (%)	Color	N-H	C-H	C-H	C=O	Other bands
11	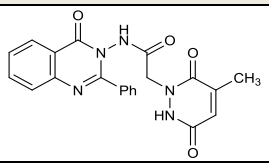	204-206	85	Grey	3429 3309	305 8	2970 2827	1737 1662	C=N 1639
12	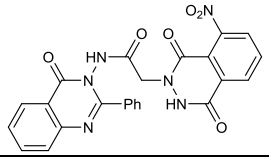	201-203	80	Brown	3427 3399	305 9	2893	1753 1662	NO_2 Asym. 1542 Sym. 1330
13	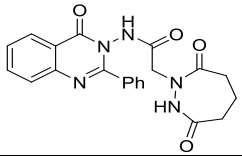	216-218	75	Brown	3434 3392	303 5	2983 2881	1733 1662	C=N 1638
14	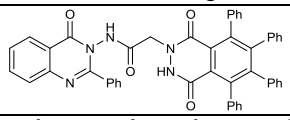	226-228	86	Pale yellow	3362	305 6	2823	1639 1662	-
15	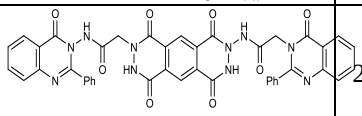	212-214	80	Gray	3307	306 6	2839	1730 1697	-

Table 9: ^{13}C NMR and ^{1}H NMR spectral data (□□□ppm) of compound (**13**)

No	Structure	^{1}H NMR spectral data	^{13}C NMR spectral data
13	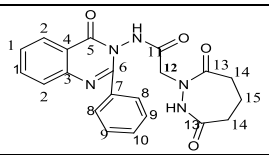	1.88-3.34 (m, 6H, CH_2), 4.70 (s, 2H, CH_2), 7.30-8.62 (m, 9H, Ar-H), 8.65 (s, 2H, N-H)	57.4 (C15), 111.4-119.0 (C1-C3, C8-C10), 120.6-122.9 (C4 and C12), 126.0 (C14), 140.2 (C6), 165.0 (C5 or C11 and C13), 174.9 (C5 or C11 and C13)

3.2. Antimicrobial activity [29]

The biological anti-microbial activities of all prepared compounds were tested against two types of bacteria [gram-positive bacteria (*S. aureus*) and gram-negative bacteria (*E. coli*)], and one type of fungus (*Candida*).

3.2.1. Antibacterial activity

In general, all the prepared compounds have shown anti-bacterial activity in comparison to the standard antibiotic (Ceftriaxone BE), which has an inhibition area of 24 nm against gram-positive bacteria and 23 nm against gram-negative bacteria, but some of the compounds showed high activity comparable to the standard antibiotic. For example, the compounds (**2**, **4**, **7**, **10**, **12**, and **13**) showed high activity against the gram-positive bacteria (*S. aureus*) with a 19-2 mm inhibition zone. Compounds (**3**, **10,** and **12**) have shown the maximum activity against gram-negative bacteria (*Escherichia coli*) in comparison to other compounds that were prepared. The inhibition zone was 18-21 mm. Compound (**12**) showed a higher activity even than the standard antibiotic used, which reached 28 and 29 mm against the gram-positive and gram-negative bacteria, respectively, as can be seen in Table 10.

3.2.2. Antifungal activity

All the prepared compounds showed higher antifungal biological activity compared to the standard antibiotic used (Flocazole), as the effectiveness of these compounds was tested against one type of fungus (*Candida albicans*). Compounds (**6**, **7**, and **12**) had the highest anti-fungal activity of 24, 26, and 25 mm, respectively. The compounds (**2**, **4**, and **9**) showed good activities of 23, 22, and 22 mm, respectively, as shown in Table 10.

Table 10: Fungal and bacterial inhibition zones in mm for compounds (**1-15**)

Compound	Inhibition zone Diameters (mm)		
	S. aureus (mm)	**E. coli (mm)**	**Candida albicans (mm)**
Ceftriaxone BE	24	23	-
Flocazole	-	-	18
Control DMSO	-	-	-
1	15	15	12
2	20	17	23
3	15	18	21
4	20	16	22
5	18	17	20
6	16	16	24
7	21	17	26
8	20	18	18
9	12	13	22
10	19	17	19
11	14	14	19
12	28	29	25
13	20	21	16
14	15	17	18
15	18	15	13

Control: 100 µg/mL, solvent: dimethyl sulfoxide

3.3. Anti-cancer activity [30]

Cytotoxic effect of three derivatives (**2**, **12** and **13**) on PC3 cancer cell line utilizing the MTT assay:

Testing of 3-(dimethylthiazol-2-yl)-2,5-diphenyl tetrazolium bromide (MTT) was carried out to conclude the cytotoxic effects of the compounds (**2**,**12** and **13**) on a human prostate *cancer cell line* (PC3). An MTT assay was carried out for the calculation of inhibition rate and cell viability on tumour cell lines with the use of a variety of concentration levels of compounds (**2**, **12** and **13**). The percentage of the treated cells viability has been estimated compared with the normal cell line WRI68. The cytotoxic effects of derivative (**2**) were tested at concentrations of 25, 50, 100, 200, and 400 µg/mL on PC3 cells. Table 11 presents a reduction in the viability of cells in a dosage-dependent pattern. Cell viability was decreased through the increase in concentration of derivative (**2**). A decrease in PC3 cell viability (%) was noted at 51.47±3.94) in the 400 µg/mL concentration. The maximum PC3 cell viability at 25.00 µg/mL had reached 95.99±0.87. A derivative (**2**) exhibited significant potent cytotoxic activities with an IC_{50} of 67.21 mg/mL. On the other hand, an IC_{50} of 179.4 mg/mL yielded from the effects of the derivative (**2**) on the WRI68 normal cell lines (Figure 1).

Table 11: Cytotoxicity effects of the derivative (**2**) on PC3 and WRI-68 cells in 24 hours post incubation at the temperature of 37 °C

Concentrations (µg/mL)	Viable cell counts of PC3 cell lines	Viable cell counts of WRI68 cell lines
	Mean ± SD	Mean ± SD
400	51.47 ± 3.94	79.98 ± 1.80
200	62.85 ± 3.42	86.00 ± 1.95
100	71.26 ± 1.54	92.21 ± 2.78
50	85.92 ± 4.14	96.49 ± 1.29
25	95.99 ± 0.87	96.95 ± 1.14

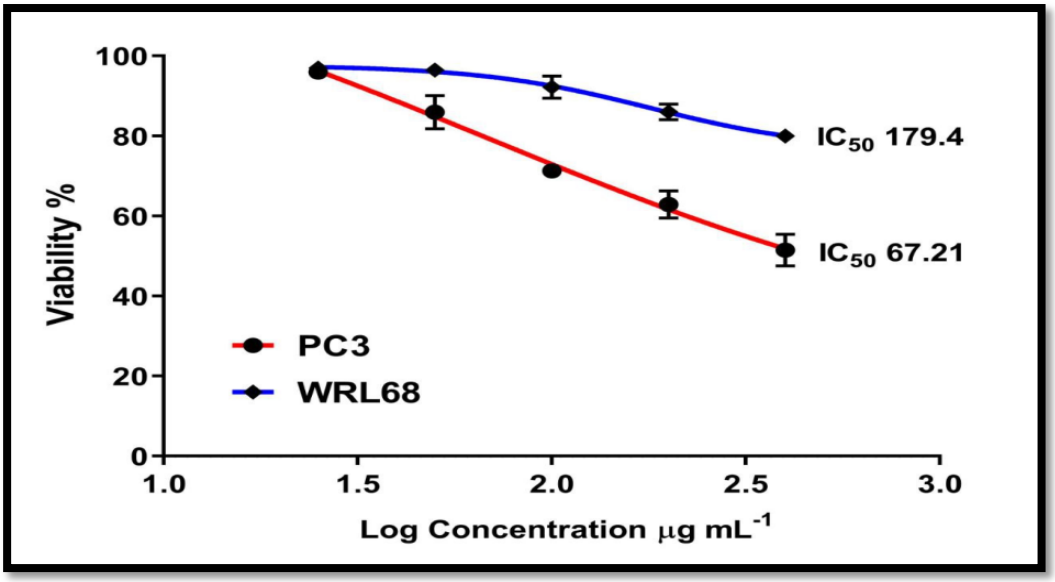

Figure 1: Representation of IC_{50} of PC3 and WRI68 cell lines of compound (**2**)

The cytotoxic effects of the derivative (**12**) in concentrations of 25, 50, 100, 200, and 400 µg/mL on PC3 cells showed a reduction of the viability of the cells in dosage-dependent patterns Table 12. The cell viability was decreased through the increase in concentrations of the derivative (**12**). A decrease in PC3 cell viability (%) was noted in the 400 µg/mL concentration (52.01±4.57). The maximum PC3 cell viability at 25 µg/mL concentration reached 95.41±1.54. A derivative (**12**) exhibited significant potent cytotoxic activity with an IC_{50} value of 90.11µg/mL concentration. On the other hand, an IC_{50} of 209.8 µg/mL was obtained from the effects of the derivative (**12**) on the WRI68 normal cell line Figure 2.

Table 12: Cytotoxicity effects of the derivative (**12**) on the PC3 and WRI-68 cells in 24 hours post incubation at 37 °C

Concentrations (mg/mL)	Viable cell counts of PC3 cell line	Viable cell counts of WRI68 cell line
	Mean ± SD	Mean ± SD
400	52.01 ± 4.57	75.58 ± 2.77
200	60.57 ± 7.64	85.65 ± 4.47
100	73.61 ± 5.40	93.98 ± 0.95
50	84.61 ± 1.25	94.29 ± 0.64
25	95.41 ± 1.54	94.98 ± 0.79

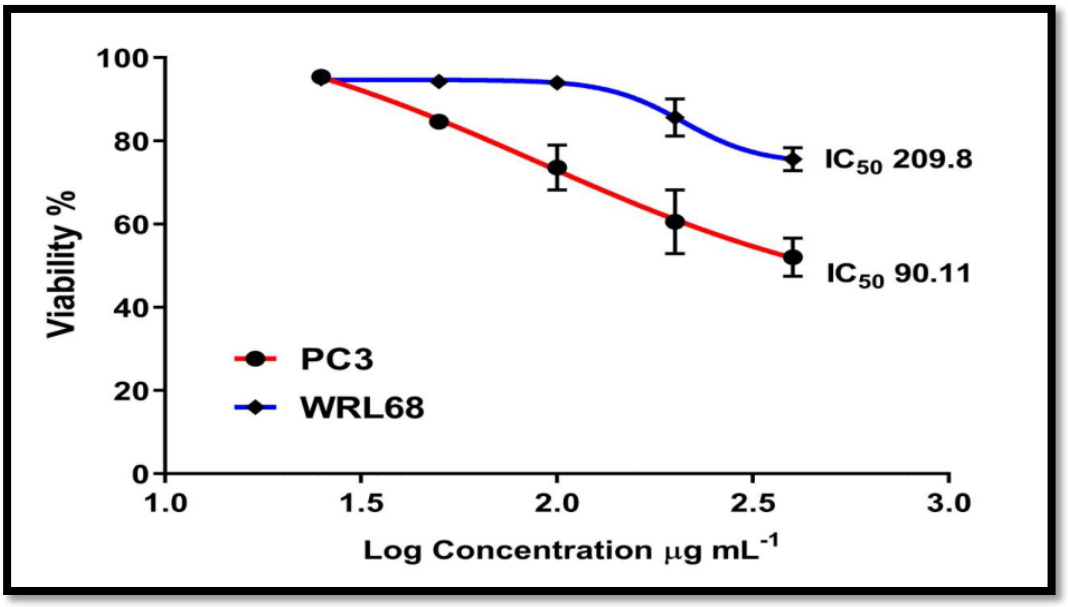

Figure 2: Representations of IC_{50} of PC3 and WRI68 cell lines of compound (**12**)

The cytotoxic effects of the derivative (**13**) at concentrations between 25.00 and 400µg/mL on the PC3 cells presented a reduction in cell viability in a dosage-dependent manner (Table 13). The cell viability decreased with the increase in concentrations of the derivative (**13**). A decrease in the PC3 cell viability (%) was noted at 400 µg/mL concentration (47.07±3.18). The maximum PC3 cell viability at 25.00µg/mL concentration had reached 86.19±2.52. A derivative (**13**) exhibited significant potent cytotoxic activities with the IC_{50} value of 80.32µg /mL. On the other hand, an IC_{50} of 117.2 µg/mL was obtained from the effects of the derivative (**13)** on the WRI68 normal cell line Figure 3.

Table 13: Cytotoxicity effects of the derivative (**13**) on the PC3 and WRI68 cells in 24 hours post incubation at a temperature of 37 °C

Concentrations (mg/mL)	Viable cell counts of PC3 cell line	Viable cell counts of WRL-68 cell line
	Mean ± SD	Mean ± SD
400	47.07 ± 3.18	69.17 ± 4.42
200	52.89 ± 2.09	74.19 ± 4.81
100	62.27 ± 1.75	84.34 ± 1.44
50	78.70 ± 1.61	93.40 ± 0.53
25	86.19 ± 2.52	95.02 ± 1.29

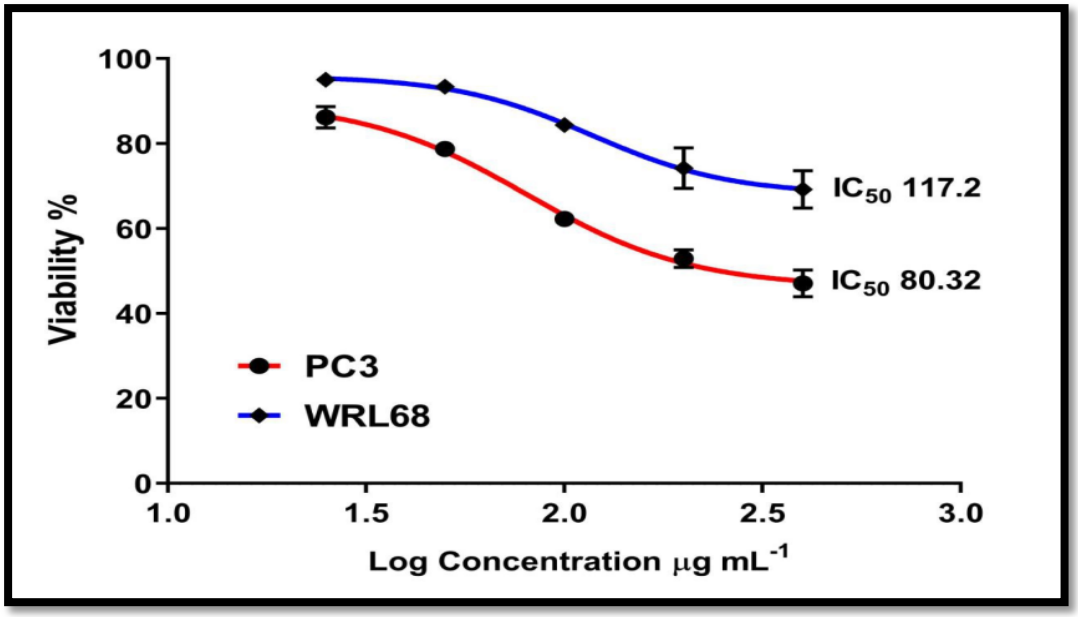

Figure 3: Representation of IC_{50} of PC3 and WRL cell lines of compound (**13)**

4. Conclusion

In this work, the synthesis of some novel pyridazine and 1,2,4-triazine derivatives starting from 2-phanyl-3-amino-quinazoline-4(3H)-one has been achieved successfully. Microdilution susceptibility testing in Muller-Hinton agar based upon the well diffusion approach was utilized for the determination of anti-bacterial and antifungal activities of newly synthesized compounds, which showed considerable antimicrobial activities. The compounds (**2**, **4**, **7**, **10**, **12**, and **13**) showed a high level of activity against the gram-positive bacteria (*S. aureus*) with a 19-28 mm inhibition zone. Compounds (**3**, **10**, and **12**) showed maximum activities against the gram-negative bacteria (*E. coli*) in comparison with the other compounds that were tested; the inhibition zone was 18-21 mm. Compound (**12**) showed a higher level of activity even than the standard antibiotic used, which reached 28 and 29 mm against the gram-positive and gram-negative bacteria, respectively. Compounds (**6**, **7**, and **12**) showed the highest anti-fungal activity at 24, 26, and 25 mm, respectively. Compounds (**2**, **4**, and **9**) showed very good activities of 23, 22, and 22 mm, respectively. Finally, compounds (**2**, **12**, and **13**) were assessed for *in vitro* cytotoxic activity against the human prostate cancer cell line PC3. These compounds showed the most potent cytotoxic activities at 400mg/mL with IC_{50} values of 67.22, 90.11, and 80.32 mg/mL, respectively.

Acknowledgements

I extend my thanks and appreciation to my esteemed professor (Prof. Dr. Suad Mohamed Hussein) for suggesting the topic of the research and for the effort she made and the valuable advice and guidance she provided, hoping that God would preserve her as an asset to support the scientific process.

References

[1] H. Greger, "Phytocarbazoles: Alkaloids with great structural diversity and pronounced biological activities", *Phytochemistry Reviews*, vol. 16, no. 6, pp. 1095-1153, 2017.

[2] P. G. Sergeev and V. G. Nenajdenko, "Recent advances in the chemistry of pyridazine-an important representative of six-membered nitrogen heterocycles", *Russian Chemical Reviews*, vol. 89, no. 4, pp. 393-382, 2020.

[3] H. A. El-Sayed and A. S. Said, "Direct synthesis of multi-functional pyrimidine, pyrazine, and pyridine scaffolds via inter-and intramolecular annulations of 3-amino-thieno[2,3-b]pyridine-2-

carboxylate", *Journal of Heterocyclic Chemistry*, vol. 56, no.3, pp.1030-1037, 2019.

[4] G. L. Points and C. M. Beaudry, "Regioselective synthesis of substituted carbazoles, bicarbazoles, and clausine C", *Organic Letters*, vol. 23, no. 17, pp. 6882-6885, 2021.

[5] X. Qian, Y. Z. Zhu, W. Y. Chang, J. Song, B. Pan, L. Lu, H. H. Gao, and J. Y. Zheng, "Benzo [a]carbazole-based donor-Π-acceptor type organic dyes for highly efficient dye-sensitized solar cells", *ACS Applied Materials and Interfaces*, vol. 7, no. 17, pp. 9015-9022, 2015.

[6] A. Malik, R. Mishra, R. Mazumder, A. Mazumder, and P. S. Mishra, "A comprehensive study on synthesis and biological activities of pyridazine derivatives", *Research Journal of Pharmacy and Technology*, vol. 14, no. 6, pp. 3423-3429, 2021.

[7] M. Imran and M. Asif, "Biologically active pyridazines and pyridazinone derivatives: A scaffold for the Highly Functionalized Compounds", *Russian Journal of Bioorganic Chemistry*, vol. 46, no. 5, pp. 726-744, 2020.

[8] E. N. Amin, A. A. Abdel-Alim, S. G. Abdel-Moty, A. N. El-Shorbagi, and M. S. H. Abdel-Rahman, "Synthesis of new 4,5-3(2H)pyridazinone derivatives and their cardiotonic, hypotensive, and platelet aggregation inhibition activities", *Archives of Pharmacal Research*, vol. 33, no.1, pp.2 5-46, 2010.

[9] E. M. Flefel, W. A. Tantawy, W. I. El-Sofany, M. El-Shahat, A. A. El-Sayed, and D. N. Abd-Elshafy, "Synthesis of some new pyridazine derivatives for anti-HAV evaluation", *Molecules (Basel, Switzerland)*, vol. 22, no. 1, pp. 148-160, 2017.

[10] Y. Zaoui, Y. Ramli, S. L. Tan, E. R. Tiekink, L. Chemlal, J. T. Mague, and M. A. Faouzi, "Synthesis, structural characterisation and theoretical studies of a novel pyridazine derivative: Investigations of anti-inflammatory activity and inhibition of α-glucosidase", *Journal of Molecular Structure*, vol. 1234, no. 1217, pp. 130177-130160, 2021.

[11] Z. X. He, Y. P. Gong, X. Zhang, L. Y. Ma, and W. Zhao, "Pyridazine as a privileged structure: An updated review on anticancer activity of pyridazine containing bioactive molecules", *European Journal of Medicinal Chemistry*, vol. 46, no. 44, pp. 2673-2678, 2021.

[12] D. Mantu, M. C. Luca, C. Moldoveanu, G. Zbancioc, and I. I. Mangalagiu, "Synthesis and antituberculosis activity of some new pyridazine derivatives. Part II", *European Journal of Medicinal Chemistry*, vol. 45, no. 11, pp. 5164-5168, 2010.

[13] H. E. Hashem, D. S. A. Haneen, K. F. Saied, and A. S. A. Youssef, "Synthesis of new annulated pyridazine derivatives and studying their antioxidant and antimicrobial activities", *Synthetic Communications*, vol. 49, no. 22, pp. 3169-3180, 2019.

[14] S. Sengmany, M. Sitter, E. Léonel, E. Le Gall, G. Loirand, T. Martens, D. Dubreuil, F. Dilasser, M. Rousselle, V. Sauzeau, J. Lebreton, M. Pipelier, and R. Le Guével, "Synthesis and biological evaluation of 3-amino-, 3-alkoxy- and 3-aryloxy-6-(hetero)arylpyridazines as potent antitumor agents", *Bioorganic and Medicinal Chemistry Letters*, vol. 29, no. 5, pp. 755-760, 2019.

[15] S. P. J. T. Bachollet, V. Vece, A. N. McCracken, B. T. Finicle, E. Selwan, N. Ben Romdhane, A. Dahal, C. Ramirez, A. L. Edinger, and S. Hanessian, "Synthetic sphingolipids with 1,2-pyridazine appendages improve antiproliferative activity in human cancer cell lines", *ACS Medicinal Chemistry Letters*, vol. 11, no. 5, pp. 686-690, 2020.

[16] M. Albratty, K. A. El-Sharkawy, and H. A. Alhazmi, "Synthesis and evaluation of some new 1,3,4-oxadiazoles bearing thiophene, thiazole, coumarin, pyridine and pyridazine derivatives as antiviral agents", *Acta pharmaceutica (Zagreb, Croatia)*, vol. 69, no. 2, pp. 261-276, 2019.

[17] A. A. Abu-Hashem, U. Fathy, and M. A. Gouda. "Synthesis of 1,2,4-triazolopyridazines, isoxazolofuropyridazines, and tetrazolopyridazines as antimicrobial agents", *Journal of Heterocyclic Chemistry*, vol. 57, no. 9, pp. 3461-3474, 2020.

[18] N. Kushwaha and C. S. Sharma, "The chemistry of triazine isomers: structures, reactions, synthesis and applications", *Mini Reviews in Medicinal Chemistry*, vol. 20, no. 20, pp. 2104-2122, 2020.

[19] H. E. Hashem, "A short review on the synthesis of 1,2,4-triazine derivatives as bioactive compounds", *Mini-Reviews in Organic Chemistry*, vol. 18, no. 8, pp. 1127-1133, 2021.

[20] Y .Y. Feng and D-H. Shiabc, "Design, synthesis and biological evaluation of quinoline-1,2,4-triazine hybrids as antimalarial agents", *Journal of Molecular Structure*, vol. 22, no. 10, pp. 133982-133970, 2022.

[21] M. S. Hussein and N. Al-Lami,"Anti-cancer and antioxidant activities of some new synthesized

mannich bases containing an imidazo(2,1-b)thiazole moiety", *Iraqi Journal of Science*, vol. 63, no. 11, pp. 4620-4636, 2022.

[22] L. Marín-Ocampo, L. A. Veloza. R. Abonia, and J. C. Sepúlveda-Arias. Anti-inflammatory activity of triazine derivatives: A systematic review, *European Journal of Medicinal Chemistry*, vol. 162, no. 12, pp. 435-447, 2019 .

[23] R. A. Alfraiji and S. M. Al-Majidi, "Synthesis, characterization and evaluation of antimicrobial activity for new heterocyclic derivatives containing pentagonal, hexagonal rings", *Iraqi Journal of Science*, vol. 55, no. 4, pp. 1694-1707, 2014.

[24] X. Tang, S. Su, M. Chen, J. He, R. Xia, T. Guo, Y. Chen, C. Zhang, J. Wang, and W. Xue. Novel chalcone derivatives containing 1,2,4-triazine moiety: design, synthesis, antibacterial and antiviral activities. *RSC Advances*, vol. 11, no. 9, pp. 6011-6020, 2019.

[25] N. J. AL-Lami, "New imidazo[2,1-d][1,3]thiazole derivatives: synthesis, antimicrobial and antifungal activity", *Iraqi Journal of Science*, vol. 56, no. 14, pp. 3274-3284, 2015.

[26] R. Pal, M. J. Akhtar, K. Raj, S. Singh, P. Sharma, S. Kalra, and B. Kumar, "Design, synthesis and evaluation of piperazine clubbed 1,2,4-triazine derivatives as potent anticonvulsant agents", *Journal of Molecular Structure*, vol. 1257, no. 1250, pp. 132587-132570, 2022.

[27] H. J. Al-Adhami and Suaad M. H. Al-Majidi, "Design, synthesis and evaluation of some new 1,2,4-triazines and 1,2-diazines derivatives of 6-amino-1,3-dimethyluracil as antimicrobial, anti-inflammatory and antioxidant activity, vol. 20, no. 02, pp. 4243-4254, 2020 .

[28] M. H. M. Al-Dahlaki and Suaad M. H. Al-Majidi, "Synthesis and study impaction antibacterial, antifungal activity newly pyridazine and 1,2,4-triazine derivatives" *Journal of Chemical Methodologies*, vol. 6, no. 4, 269-279, 2022.

[29] L. Ma, H. Wang, J. Wang, L. Liu, S. Zhang, and M. Bu, Novel steroidal 5α,8α-endoperoxide derivatives with semicarbazone/thiosemicarbazone side-chain as apoptotic inducers through an intrinsic apoptosis pathway: design, synthesis and biological studies; *Molecules*, vol. 25, no. 5, pp. 1-16, 2020.

[30] L. Gourdon, K. Cariou and G. Gasser, Phototherapeutic anticancer strategies with first-row transition metal complexes: a critical review, *Chemical Society Reviews*, vol. 51, no. 3, pp. 1167-1195, 2022.